

Cosmological properties of a class of Λ decaying cosmologies

V. Silveira^{1,3} and I. Waga^{2,3}

¹*Universidade de Brasília, International Centre of Condensed Matter Physics, C. P. 04513, 70919-970, Brazil.*

²*Universidade Federal do Rio de Janeiro, Instituto de Física, C. P. 68528, 21945-970, Brazil.*

³*NASA/Fermilab Astrophysics Center, Fermi National Accelerator Laboratory, Batavia, IL, 60510*

(May 16, 2018)

We investigate some properties of flat cosmological models with a Λ term that decreases with time as $\Lambda \propto a^{-m}$ (a is the scale factor and m is a parameter $0 \leq m < 3$). The models are equivalent to standard cosmology with matter and radiation plus an exotic fluid with the equation of state $p_x = (m/3 - 1)\rho_x$. We study the effect of the decaying Λ term on the cosmic microwave background anisotropy and by using a seminumeric method we compute the angular power spectrum (up to $l = 20$) for different values of m and Ω_{m0} . We also investigate the constraints imposed on the models by the magnitude-redshift test in which high-redshift type Ia supernovae (SNe Ia) are used as standard candles. We obtain the 95.4%, 90%, and 68% confidence levels on the parameters m and Ω_{m0} and compare them with those arising from lensing statistics. Our analysis reveals that the SNe Ia constraints are stronger for low values of m and Ω_{m0} , while those from lensing statistics are more important for $m \gtrsim 1$. Models with $\Omega_{m0} \gtrsim 0.2$ and $m \gtrsim 1.6$ are in good agreement with the data.

PACS number(s): 98.80.Hw

I. INTRODUCTION

Flat cosmological models with a cosmological constant are currently serious candidates to describe the dynamics of the universe. There are three main reasons for the present interest on these models. First, they can reconcile inflation with dynamic estimates for the density parameter (Ω). Observations indicate $\Omega_{m0} = 0.2 - 0.4$ for matter that clumps on scales $20 - 30h^{-1}$ Mpc, while inflationary models usually predict $\Omega_{total} = 1$. Second, these models, when normalized by data from the Cosmic Background Explorer (COBE) predict less power in the perturbation spectrum at small scales than standard cold dark matter (CDM), in accordance with observations [1]. The third motivation for introducing a cosmological constant is the “age crisis.” In flat models with $\Omega_{m0} = 1$ only if $h < 0.57$ (h is the present value of the Hubble parameter in units of $100 \text{ km/s Mpc}^{-1}$) is it possible to get theoretical ages for the universe that are higher than the lowest values (~ 12 Gyear) estimated for the galactic globular cluster system [2]. However, current estimates based on observations of Cepheids stars in the Virgo cluster and type Ia supernovae indicate higher values for h [3].

In the past the cosmological constant was introduced and, with the improvement of the observational data,

later discarded. Now, however, the situation may change. By taking into account the vacuum contribution to the energy-momentum tensor we can define an effective cosmological constant (Λ_{eff}) that is the sum of two terms, the bare cosmological term and $8\pi G\rho_{vac}$ (ρ_{vac} is the vacuum energy density). From quantum field theory we should expect $\rho_{vac} \sim M_{Pl}^4$ (M_{Pl} is the Planck mass), or perhaps another energy density related to some spontaneous symmetry-breaking scale such as M_{SUSY} or M_{weak} to the fourth power. The problem lies in that these values are enormous when compared with astronomical bounds for $\rho_{\Lambda_{eff}}$. Extreme fine-tuning between $8\pi G\rho_{vac}$ and the bare Λ is necessary to make theory compatible with observations.

One possible explanation for a small Λ term is to assume that it is dynamically evolving and not constant, that is, as the universe evolves from an earlier hotter and denser epoch, the effective cosmological term also evolves and decreases to its present value [4]. There are also strong observational motivations for considering cosmological models with a decreasing Λ term instead of a constant one. Usually in a dynamical- Λ cosmological model, the distance to an object with redshift z is smaller than the distance to the same object in a constant- Λ model with the same value of the density parameter. As we shall discuss in Sec. IV, this implies that constraints coming from lensing statistics and from high redshift supernovae can be considerably weaker in these models [18].

Recently [5] we suggested a class of models in which Λ decreases as $\Lambda \propto a^{-m}$ [here a is the scale factor of the Friedman-Robertson-Walker (FRW) metric and m is a constant ($0 \leq m < 3$)]. Although Chen and Wu [6] gave some interesting arguments favoring the special value $m = 2$, it is clear that the above functional dependence with the scale factor is only phenomenological and does not come from particle physics first principles. However, we believe it deserves further investigation for the following reasons. First, these models generalize several other models present in the literature. So, by investigating their properties we are studying at once the models they generalize. Second, since $m < 3$ the universe age in these models is always larger than the age obtained in the standard Einstein-de Sitter cosmology and if $m < 2$ the age is larger than the one we get in an open model with the same Ω_{m0} . This is an important aspect if we are interested in solving the “age problem.” Further, since $m < 4$ the Λ term is generally not important during the radiation-dominated phase and nucleosynthesis proceed

as in the standard model [7]. Finally, the models are mathematically simple and in most cases can be treated analytically.

This paper is organized as follows. In Sec. II the basic equations of the models are obtained and our main assumptions presented. In Sec. III we investigate the effect of the Λ term on the cosmic microwave background (CMB) anisotropy and compute the angular power spectrum for small values of l for different values of the parameter m and Ω_{m0} . Constraints on the models from high redshift SNe Ia and from lensing statistics are obtained in Sec. IV.

II. THE MODELS AND THE FIELD EQUATIONS

In this paper we consider spatially flat, homogeneous, and isotropic cosmologies with a time-dependent Λ term:

$$\Lambda = 8\pi G\rho_\nu = 3\alpha a^{-m}. \quad (2.1)$$

Here the parameters α and m are restricted to the range $0 \leq m < 3$, $\alpha \geq 0$ and the factor 3 was only introduced for mathematical convenience. We consider the cosmic fluid to be a mixture of nonrelativistic matter and radiation ($p_r = \frac{1}{3}\rho_r$) with a perfect fluid energy momentum tensor,

$$T^\mu{}_\nu = T_r^\mu{}_\nu + T_m^\mu{}_\nu = \text{diag}(\rho, -p, -p, -p), \quad (2.2)$$

where $\rho = \rho_r + \rho_m$ is the total energy density (radiation plus nonrelativistic matter) and $p = p_r$ is the thermodynamic pressure.

As in Ref. [5] we assume that vacuum decays only into relativistic particles, such that the nonrelativistic matter energy momentum tensor is conserved ($\rho_m \propto a^{-3}$). The radiation energy density has two parts: one conserved, $\Omega_{r0}H_0^2(a_0/a)^4$, $\Omega_{r0} = 4.3 \times 10^{-5}h^{-2}$, and a second one, $\frac{3m\alpha}{8\pi G(4-m)}a^{-m}$, which arises due to the vacuum decay. Here a_0 is the present value of the scale factor and H_0 is the present value of the Hubble parameter. In the following, subscripts 0 will always indicate present values.

The Einstein equations for the models we are considering reduce to two equations: namely,

$$\begin{aligned} \left(\frac{\dot{a}}{a}\right)^2 &= \Omega_{m0}H_0^2\left(\frac{a_0}{a}\right)^3 + \Omega_{r0}H_0^2\left(\frac{a_0}{a}\right)^4 \\ &+ \Omega_{x0}H_0^2\left(\frac{a_0}{a}\right)^m \end{aligned} \quad (2.3)$$

and

$$\begin{aligned} \frac{\ddot{a}}{a} &= -\frac{1}{2}\Omega_{m0}H_0^2\left(\frac{a_0}{a}\right)^3 - \Omega_{r0}H_0^2\left(\frac{a_0}{a}\right)^4 \\ &+ \frac{(2-m)}{2}\Omega_{x0}H_0^2\left(\frac{a_0}{a}\right)^m, \end{aligned} \quad (2.4)$$

where Ω_{m0} is the matter density parameter and $\Omega_{x0} = \frac{4\alpha H_0^{-2} a_0^{-m}}{(4-m)}$.

The above equations are quite general and apply for a broad spectrum of models. For instance, if $m = 0$, the usual flat FRW model with a cosmological constant is obtained. If we take $m = 2$, Eqs. (2.3) and (2.4) assume the same form of the Einstein equations for open models and also appear in some string-dominated cosmologies [8]. Further, we would obtain the *same* Einstein equations if, instead of a cosmological term, we would have considered (beside conserved matter and radiation) an exotic x fluid with equation of state, $p_x = \left(\frac{m}{3} - 1\right)\rho_x$ [9]. All we discuss here also applies for these cosmologies and to emphasize this point in the following we shall use the expression “x component” to interchangeably designate the Λ term or the x fluid.

III. THE ANGULAR POWER SPECTRUM

The evolution of perturbations in the models we are considering may be studied considering two different phases [5]. For $a < a_M = a_0\left(\frac{\Omega_{m0}}{\Omega_{x0}}\right)^{\frac{1}{4-m}}$, the energy density of the universe is dominated by radiation and/or matter, and the contribution from the x component may be neglected. During the second phase, characterized by $a > a_M$, the energy density of the universe is dominated by nonrelativistic matter and/or the x component. In this phase, the x component contribution becomes more and more important and the deviations from the usual matter-dominated cosmological model increase as the universe expands.

To describe the perturbation growth in these two phases, we consider the usual linear perturbation theory. Each Fourier component of the perturbation, $\delta_k(t)$, grows independently of the other modes and may be related to the primordial power spectrum with the help of the transfer function:

$$\delta_k(t) = T(k)\delta_k(t_i), \quad (3.1)$$

where $\delta_k(t_i)$ is the primordial spectrum, usually taken to be

$$|\delta_k(t_i)|^2 = Ak^n. \quad (3.2)$$

In (3.1) $T(k)$ is the transfer function, which incorporates all deformations undergone by the k -mode perturbation and t may be any time $t > t_i$. If the initial perturbation is adiabatic and $n = 1$ we have a primordial scale invariant adiabatic perturbation that is usually predicted by inflationary models. In fact, for flat models without a cosmological constant it can be shown that, in this case, the quantity $k^3 |\delta_k|^2$ at $t = t_{enter}$, is independent of k for any k . Here, t_{enter} is the instant when the perturbation crosses the Hubble radius. However, this is not necessarily true if we have a cosmological term. In [5] we adopted a true scale invariant Harrison-Zeldovich spectrum for the models we are analyzing. Here we shall use the primordial scale invariant spectrum as defined above.

The power spectrum is defined in the standard way by $P(k) = |\delta_k(t_0)|^2$ where t_0 is the present time. For flat models with $\Lambda = 0$, and after radiation-matter equality ($a > a_{eq}$), all modes, inside and outside the Hubble radius, evolve in the very same way. So, $\delta_k(t)$, in fact, does not experience any deformation for $t > t_{eq}$ and $P(k)$ reflects the power spectrum for any $t > t_{eq}$. Since in our model $a_{eq} < a_M$, the evolution during the first phase, dominated by radiation and matter, may be described by simply taking the standard power spectrum at $a = a_M$, with the transfer function as computed by Bond and Efstathiou [10]:

$$T(k) = (1 + (ak + (bk)^{3/2} + (ck)^2)^\nu)^{-\frac{1}{\nu}} \quad (3.3)$$

where $a = 6.4(\Omega h^2)^{-1}$ Mpc, $b = 3.0(\Omega h^2)^{-1}$ Mpc, $c = 1.7(\Omega h^2)^{-1}$ Mpc, and $\nu = 1.13$.

After radiation and x component equality, $a > a_M$, the increasingly importance of the x component energy density must be taken into account. To describe the perturbations after a_M , we consider the evolution of matter perturbations in the background dominated by matter and the x component. We shall use the approximation that the x component is smooth. In this case it can be shown [11] that all modes, inside and outside the Hubble radius, grow at the same rate as in a flat universe dominated by nonrelativistic particles. So again no extra deformation is introduced in the power spectrum by the presence of the x component and, to study the multipole expansion of the power spectrum, we are allowed to use the transfer function given by Eq. (3.3).

Since one of our goals is to understand the effect of the decaying cosmological term (x component) on the CMB anisotropy, we consider the relation between the mass density perturbation and the fractional perturbation to the CMB temperature $\frac{\delta T}{T}$. Almost 30 years ago, Sachs and Wolfe [12] obtained the expression relating fluctuations in the gravitational potential on the last scattering surface with CMB temperature anisotropies on large angular scales ($\theta \gg 1$ deg). For a flat universe their formula can be written as [13]

$$\begin{aligned} \frac{\delta T}{T} = & - \left[\frac{a}{2} \frac{dD}{dt} \frac{\partial k}{\partial x^\alpha} \gamma^\alpha \right]_{t_{em}}^{t_{ob}} - \left[\frac{a}{2} \frac{d}{dt} \left(a \frac{dD}{dt} \right) k \right]_{t_{em}}^{t_{ob}} \\ & + \frac{1}{2} \int_{t_{em}}^{t_{ob}} dt k \frac{d}{dt} a \frac{d}{dt} a \frac{dD}{dt}, \end{aligned} \quad (3.4)$$

where $D(t)$ describes the time dependence of the growing mode of δ_m , $\delta_m(\vec{x}, t) = A(\vec{x})D(t)$, γ^α is the unit vector pointing along a null ray from the observer to the source, and where $k(\vec{x})$ is given by

$$k(\vec{x}) = -\frac{1}{2\pi} \int \frac{\delta_m(\vec{x}', t)}{D(t)} \frac{d^3 x'}{|\vec{x} - \vec{x}'|}. \quad (3.5)$$

The first term in the right-hand side (RHS) of (3.4) describes the anisotropy caused by the relative motion

source observer. The effect of the observer's motion may be systematically removed from the experimental data, and will not be considered any further. The effect of the source motion is a Doppler contribution related to velocity perturbations on the last scattering surface and cannot be eliminated. The second term in Eq. (3.4) includes the usual Sachs-Wolfe effect (SW) and a constant part evaluated at the present epoch which does not contribute to the observed anisotropy. Finally, there is the last term, usually called the integrated Sachs-Wolfe effect (ISW), which represents the redshift or blueshift of the photon energy caused by its traveling through regions of space with time-varying gravitational potential. Note that during the radiation-matter domination phase the growing modes behave as [5]

$$D(a) = D_{dec} \left(1 + \frac{3a_{dec}}{2a_{eq}}\right)^{-1} \left(1 + \frac{3a}{2a_{eq}}\right), \quad (3.6)$$

where $a_{eq} = a_0 \frac{\Omega_{r0}}{\Omega_{m0}}$ is the scale factor at matter-radiation energy density equality. So, since in flat models, during the radiation domination, we have $a \propto t^{1/2}$, and during matter domination the scale factor grows as $a \propto t^{2/3}$, it is easy to see that the contribution of the last term in Eq. (3.4) vanishes in both cases. This reflects the fact that, during these eras, the gravitational potential is time independent. However, during the x component domination, the gravitational potential will not be constant and the ISW term will no longer be zero. In fact its contribution may be of the same order of the usual SW term for the lower modes in the harmonic expansion. In order to study the CMB anisotropies in the models described above, we keep three contributions in the RHS of (3.4): SW, ISW, and Doppler.

The full temperature correlation function is defined by

$$C(\alpha) = \left\langle \frac{\Delta T}{T}(\hat{n}) \frac{\Delta T}{T}(\hat{m}) \right\rangle_{\hat{n} \cdot \hat{m} = \cos(\alpha)} \quad (3.7)$$

where $\langle \dots \rangle$ denotes an average over all positions \vec{x} and all directions \hat{n} , \hat{m} separated by an angle α .

To compute the average value in Eq. (3.7), we first analyze the ISW contribution [14]. We have

$$\begin{aligned} C^{ISW}(\alpha) = & \int_{a_M}^{a_0} da \int_{a_M}^{a_0} da' G(a) G(a') \int \frac{d^3 k}{(2\pi)^3} \\ & \times \int \frac{d^3 k'}{(2\pi)^3} \frac{\delta_k \delta_{k'}^*}{k^2 k'^2} \langle e^{i(\vec{k}' - \vec{k}) \cdot \vec{x}_0} \rangle_{x_0} \\ & \times \langle e^{-i\vec{k} \cdot \hat{n} I_2(a, a_0) + i\vec{k}' \cdot \hat{m} I_2(a', a_0)} \rangle_{\hat{n} \cdot \hat{m} = \cos(\alpha)}. \end{aligned} \quad (3.8)$$

Here

$$I_2(a, a_0) = \frac{1}{H_0} \int_a^{a_0} \frac{dx}{\sqrt{\Omega_{m0} x + (1 - \Omega_{m0}) x^{4-m}}}, \quad (3.9)$$

and

$$G(a) = - \left(\frac{3D}{a} - D'(3 + \frac{m}{2} (\frac{a_d}{a})^{m-3}) \right) H_0^2 \Omega_{m0} a^2 (\frac{a_0}{a})^3, \quad (3.10)$$

where $a_d = a_0 (\frac{\Omega_{m0}}{\Omega_{x0}})^{1/(3-m)}$ and $D' = dD/da$. Note that if $m = 0$ and $D \propto a$ we obtain $G(a) = 0$. Equation (3.8) was obtained by making use of the field Eqs. (2.3) and (2.4), with $\Omega_{r0} = 0$, and the time evolution differential equation for D ,

$$\ddot{D} + 2\frac{\dot{a}}{a}\dot{D} - 4\pi G\rho_m D = 0. \quad (3.11)$$

By using that,

$$\begin{aligned} \langle e^{i(\vec{k}' - \vec{k}) \cdot \vec{x}_0} \rangle_{x_0} &= \frac{1}{V} \int d^3 x_0 e^{i(\vec{k}' - \vec{k}) \cdot \vec{x}_0} \\ &= \frac{(2\pi)^3}{V} \delta^3(\vec{k}' - \vec{k}) \end{aligned} \quad (3.12)$$

and

$$\begin{aligned} &\langle e^{-i\vec{k} \cdot \hat{n} I_2(a, a_0) + i\vec{k}' \cdot \hat{m} I_2(a', a_0)} \rangle_{\hat{n} \cdot \hat{m} = \cos(\alpha)} \\ &= j_0 \left[k \left(I_2(a, a_0)^2 + I_2(a', a_0)^2 \right. \right. \\ &\quad \left. \left. - 2I_2(a, a_0) I_2(a', a_0) \cos(\alpha) \right)^{1/2} \right], \end{aligned} \quad (3.13)$$

where $j_0(x) = \frac{\sin(x)}{x}$, we reduce (3.8) to

$$\begin{aligned} C^{ISW}(\alpha) &= \int_0^\infty \frac{dk}{2\pi^2} \frac{P(k)}{k^2} \int_{a_M}^{a_0} da \int_{a_M}^{a_0} da' G(a) G(a') \\ &\times j_0 \left[k \left(I_2(a, a_0)^2 + I_2(a', a_0)^2 \right. \right. \\ &\quad \left. \left. - 2I_2(a, a_0) I_2(a', a_0) \cos(\alpha) \right)^{1/2} \right], \end{aligned} \quad (3.14)$$

where $P(k) = AkT(k)^2$. Analogously we obtain

$$\begin{aligned} C^{SW}(\alpha) &= \left(\frac{3H_0^2 \Omega_{m0} D_{dec} a_0^3}{4a_{eq}(1 + \frac{3}{2} a_{dec}/a_{eq})} \right)^2 \times \\ &\int_0^\infty \frac{dk}{2\pi^2} \frac{P(k)}{k^2} j_0[2k (I(a_{dec}, a_0)) \sin(\alpha/2)], \end{aligned} \quad (3.15)$$

where $I(a_{dec}, a_0) = I_1(a_{dec}, a_M) + I_2(a_M, a_0)$, with

$$I_1(a_{dec}, a) = \frac{1}{H_0} \int_{a_{dec}}^a \frac{dx}{\sqrt{\Omega_{m0} x + (1 - \Omega_{m0})}}. \quad (3.16)$$

The Doppler term is given by

$$\begin{aligned} C^{Dop}(\alpha) &= a_{dec}^2 \dot{D}_{dec}^2 \int_0^\infty \frac{dk}{2\pi^2} \frac{P(k)}{k^2} \times \\ &\frac{d}{dx} \frac{d}{dy} \left(j_0[k \sqrt{x^2 + y^2 - 2xy \cos(\alpha)}] \right)_{x=y=I(a_{dec}, a_0)}. \end{aligned} \quad (3.17)$$

The cross terms reduce to

$$\begin{aligned} C^{ISW-SW}(\alpha) &= \\ &- \frac{3H_0^2 \Omega_{m0} D_{dec} a_0^3}{2a_{eq}(1 + \frac{3}{2} a_{dec}/a_{eq})} \int_{a_M}^{a_0} da G(a) \int_0^\infty \frac{dk}{2\pi^2} \frac{P(k)}{k^2} \\ &\times j_0[k \left(I(a_{dec}, a_0)^2 + I_2(a, a_0)^2 \right. \\ &\quad \left. - 2I(a_{dec}, a_0) I_2(a, a_0) \cos(\alpha) \right)^{1/2}] \end{aligned} \quad (3.18)$$

$$\begin{aligned} C^{Dop-SW}(\alpha) &= \left(\frac{3H_0^2 \Omega_{m0} \dot{D}_{dec} D_{dec} a_0^3}{(\frac{a_{eq}}{a_{dec}} + \frac{3}{2})} \right) \\ &\times \int_0^\infty \frac{dk}{2\pi^2} \frac{P(k)}{k^2} \frac{d}{dx} \left(j_0[k(x^2 + I(a_{dec}, a_0)^2 \right. \\ &\quad \left. - 2xI(a_{dec}, a_0) \cos(\alpha))^{1/2}] \right)_{x=I(a_{dec}, a_0)} \end{aligned} \quad (3.19)$$

$$\begin{aligned} C^{Dop-ISW}(\alpha) &= -2a_{dec} \dot{D}_{dec} \int_{a_M}^{a_0} da G(a) \\ &\times \int_0^\infty \frac{dk}{2\pi^2} \frac{P(k)}{k^2} \frac{d}{dx} \left(j_0[k(x^2 + I(a, a_0)^2 \right. \\ &\quad \left. - 2xI(a, a_0) \cos(\alpha))^{1/2}] \right)_{x=I(a_{dec}, a_0)} \end{aligned} \quad (3.20)$$

The total contribution to (3.7) may be written as

$$\begin{aligned} C(\alpha) &= C^{ISW} + C^{SW} + C^{Dop} + C^{ISW-SW} \\ &\quad + C^{Dop-SW} + C^{Dop-ISW} \end{aligned} \quad (3.21)$$

It is convenient to expand the temperature correlation function in angular multipoles, using Legendre Polynomials $P_l(\cos(\alpha))$:

$$C(\alpha) = \sum_{l=0}^{\infty} \frac{2l+1}{4\pi} P_l(\cos(\alpha)) C_l \quad (3.22)$$

and $C_l = 2\pi \int_{-1}^1 d\cos(\theta) P_l(\cos(\theta)) C(\theta)$. With the help of the relation $j_0[k\sqrt{r^2 + q^2 - 2rq\cos(\theta)}] = \sum_{n=0}^{\infty} (2n+1) P_n(\cos(\theta)) j_n[kr] j_n[kq]$, where $j_l[x]$ is a spherical Bessel function, the integrals in the contributions for C_l decouple and the angular power spectrum becomes

$$\begin{aligned} C_l &= C_l^{ISW} + C_l^{SW} + C_l^{Dop} + C_l^{ISW-SW} \\ &\quad + C_l^{Dop-SW} + C_l^{Dop-ISW} \end{aligned} \quad (3.23)$$

with

$$C_l^{ISW} = \frac{2}{\pi} \int_0^\infty \frac{dk}{k^2} P(k) (X_l(k))^2 \quad (3.24)$$

where

$$X_l(k) = \int_{a_M}^{a_0} da G(a) j_l[kI(a, a_0)], \quad (3.25)$$

$$\begin{aligned} C_l^{SW} &= \frac{2}{\pi} \left(\frac{3H_0^2 \Omega_{m0} D_{dec} a_0^3}{4a_{eq}(1 + \frac{3}{2} a_{dec}/a_{eq})} \right)^2 \\ &\times \int_0^\infty \frac{dk}{k^2} P(k) j_l^2[kI(a_{dec}, a_0)], \end{aligned} \quad (3.26)$$

$$C_l^{Dop} = \frac{2}{\pi} a_{dec}^2 \dot{D}_{dec}^2 \times \int_0^\infty \frac{dk}{k^2} P(k) \left(\frac{d}{dx} (j_l[kx])_{x=I(a_{dec}, a_0)} \right)^2, \quad (3.27)$$

$$C_l^{ISW-SW} = -\frac{3H_0^2 \Omega_{m0} D_{dec} a_0^3}{\pi a_{eq} (1 + \frac{3}{2} a_{dec}/a_{eq})} \times \int_0^\infty \frac{dk}{k^2} P(k) j_l[kI(a_{dec}, a_0)] X_l(k), \quad (3.28)$$

$$C_l^{Dop-SW} = \left(\frac{3H_0^2 \Omega_{m0} \dot{D}_{dec} D_{dec} a_0^3}{\pi (\frac{a_{eq}}{a_{dec}} + \frac{3}{2})} \right) \int_0^\infty \frac{dk}{k^2} P(k) \times j_l[kI(a_{dec}, a_0)] \frac{d}{dx} (j_l[kx])_{x=I(a_{dec}, a_0)}, \quad (3.29)$$

and

$$C_l^{Dop-ISW} = -\frac{4a_{dec} \dot{D}_{dec}}{\pi} \times \int_0^\infty \frac{dk}{k^2} P(k) X_l(k) \frac{d}{dx} (j_l[kx])_{x=I(a_{dec}, a_0)}. \quad (3.30)$$

Using the expressions above, we compute the angular power spectrum for different values of m and Ω_{m0} . Calculations are done in a semianalytical way through the following steps. To make the integration in $X_l(k)$ [Eq. (3.25)], we change variables. By defining $w = I(a, a_0)$, and by using an interpolated polynomial, we rewrite the integral in the new w variable as

$$X_l = - \int_0^{w_M} dw CI(w) j_l[kw]. \quad (3.31)$$

Here $CI(w)$ is an interpolated polynomial, which replaces the function $C(w) = \frac{d}{dw} (I^{-1}(w)) G(I^{-1}(w))$, where $I^{-1}(w)$ stands for the inverse of $w = I(a, a_0)$. The precision of this interpolation may be estimated by comparing $CI(w)$ and the original function $C(w)$. In the models we consider, this comparison shows that using the seventh-order interpolated polynomial, $CI(w) = \sum_{n=0}^7 a_n w^n$, introduces an error always smaller than 0.07%. With the help of this approximation, the resulting seven integrals in X_l can be analytically computed. The form of these expressions remains the same for all models that we want to consider. Changing among models only changes the numerical values of a_n together with the upper limit in the integral, w_M . Once we have calculated these auxiliary functions $X_l(k)$, we may compute the coefficients in Eqs. (3.24), (3.28), and (3.30) by direct integration in k . In the limit $k \rightarrow 0$, the integrand is well behaved. For large values of k , the integrand decreases very fast. However, while decreasing, these integrands oscillate wildly, making the integral procedure slower and slower. To avoid this technical difficulty, we truncate the integral at some value of k , and we certify

ourselves that the truncation is affecting our results in a controlled way. For values of k larger than the truncation value, we compute the integrals replacing the oscillating $j_l(kI)$ by an envelope function, and the result of these integrals is taken as an upper bound of the error introduced by the truncation in k . This error grows steadily with l , starting with 0.03% for $l = 2$ and growing up to the range 2–3% for $l = 20$ and different values of m .

The numerical results obtained with the method described above are plotted in Figs. 1 and 2.

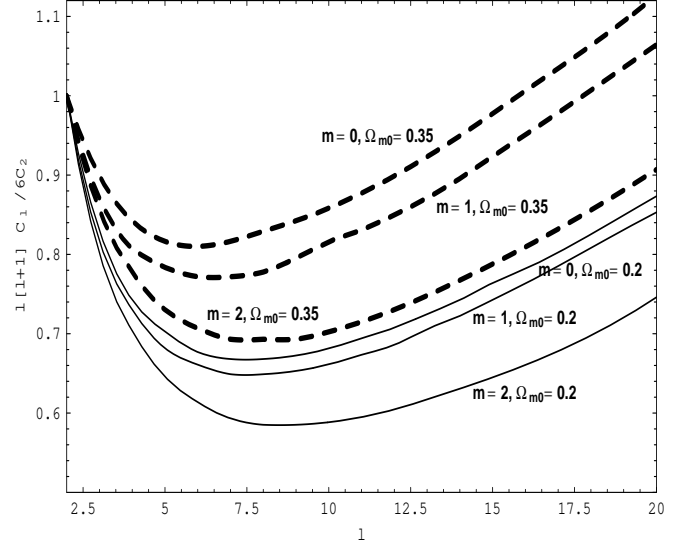


FIG. 1. The angular power spectrum $l(l+1)C_l/6C_2 \times l$ is shown for different values of m and Ω_{m0} .

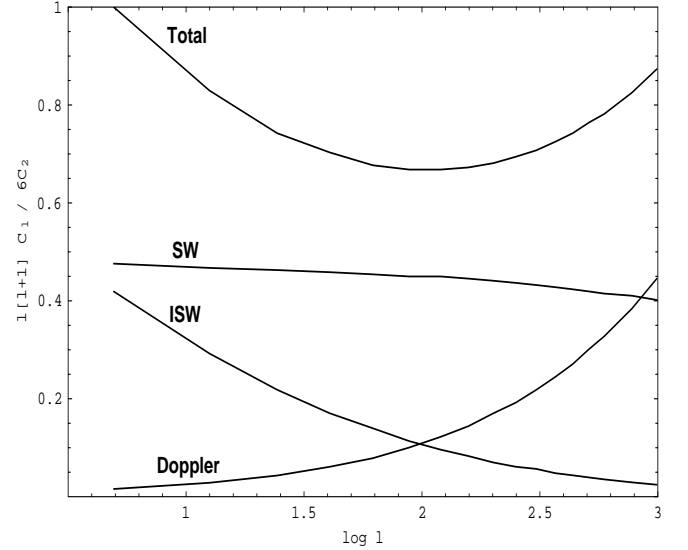


FIG. 2. The Doppler, the Sachs-Wolfe, and the integrated Sachs-Wolfe contributions to the angular power spectrum are shown. For the figure we considered the special model for which $m = 2$ and $\Omega_{m0} = 0.2$.

In Fig. 2 we plot for $m = 2$ and $\Omega_{m0} = 0.2$ the separate

contributions from the Sachs-Wolfe, Doppler and integrated Sachs-Wolfe effects. Crossed terms are not shown. Basically, in the range $2 \leq l \leq 20$, the Sachs-Wolfe contribution remains always important, with a slight decrease. The integrated Sachs-Wolfe is large for small values of l , but soon it becomes unimportant, reducing to just 2% of C_l at $l = 20$. On the other hand, the Doppler contribution starts very small and grows fast to become the dominant contribution at $l = 20$.

For the analyzed models, the curves $l(l+1)C_l/6C_2 \times l$ in Fig. 1, show a common feature, a minimum for small values of l . We see that, for fixed Ω_{m0} and h , the position of this minimum changes with m , becoming deeper as m grows larger. This feature reflects the fact that the contribution from the ISW effect is larger for larger values of the parameter m . We also observe that for fixed m and h and different values of the matter content, the minimum grows deeper for smaller values of Ω_{m0} . Again this feature agrees with the fact that it is the x component term which brings up the nonzero ISW effect, which, by its turn, makes the minimum deeper. So, since $\Omega_{total} = 1$, less nonrelativistic matter means more x component contribution, more ISW effect, and consequently deeper minimum.

IV. CONSTRAINTS FROM HIGH-REDSHIFT TYPE IA SUPERNOVAE AND LENSING STATISTICS

The Supernovae Cosmology Project is an ongoing program to systematically search and study high- z supernovae. In a recent report [15] Perlmutter *et al.* analyzed seven SNe (with redshift $z = 0.35 - 0.46$), of more than 28 supernovae discovered, and obtained constraints on cosmological parameters, specially on the cosmological constant. Their preliminary result, $\Omega_\Lambda < 0.51$ at the 95% confidence level, strongly constraints models for the universe with a cosmological constant. In this section we use their observational results and adapt their procedure to constraint the class of models described in Sec. II.

The basic idea is to use type Ia supernovae as standard candles for the classic magnitude-redshift test. As in [15] we express the apparent bolometric magnitude $m(z)$ as

$$m(z) = \mathcal{M} + 5 \log d_l(z, \Omega_{m0}, m) \quad (4.1)$$

where in our case the luminosity distance (in units of H_0^{-1}) is given by,

$$d_l(z, \Omega_{m0}, m) = c(1+z) \times \int_0^z \frac{dz}{\sqrt{(1+z)^3 \Omega_{m0} + (1+z)^m (1-\Omega_{m0})}} \quad (4.2)$$

In Eq. (4.1)

$$\mathcal{M} = M - 5 \log H_0 + 25 \quad (4.3)$$

is the “zero point” magnitude (or Hubble intercept magnitude), which is estimated from the apparent magnitude and redshift of low-redshift ($z < 0.1$) SNe Ia. The nearby supernovae data set used by Perlmutter *et al.* in the determination of \mathcal{M} were those 18 SNe Ia, discovered by the Calan/Tololo Supernovae Search [16] for which the first observations were made no later than 5 days after maximum.

Although SNe Ia are very similar explosion events, it is now known that they do not constitute a completely homogeneous class. Recently progress was made in the study of their inhomogeneities. Phillips [17] showed that there is a correlation between absolute magnitudes (M) at maximum light and the initial decline parameter Δm_{15} , the B-magnitude decline in the first 15 days after maximum. By studying the Calan/Tololo type Ia supernovae, Hamuy *et al.* [16] confirmed the existence of the correlation suggested by Phillips and obtained a prescription for correcting observed B-magnitudes to make them comparable to an arbitrary “standard” SNe Ia light curve of width $\Delta m_{15} = 1.1$. After adding the correction to the SNe Ia low- z set they reduced the magnitude dispersion from 0.26 to $\sigma_{M_{B,corr}}^{Hamuy} = 0.17$. Perlmutter *et al.* did the same for the seven high- z supernovae and reduced the dispersion from 0.27 to 0.19 mag.

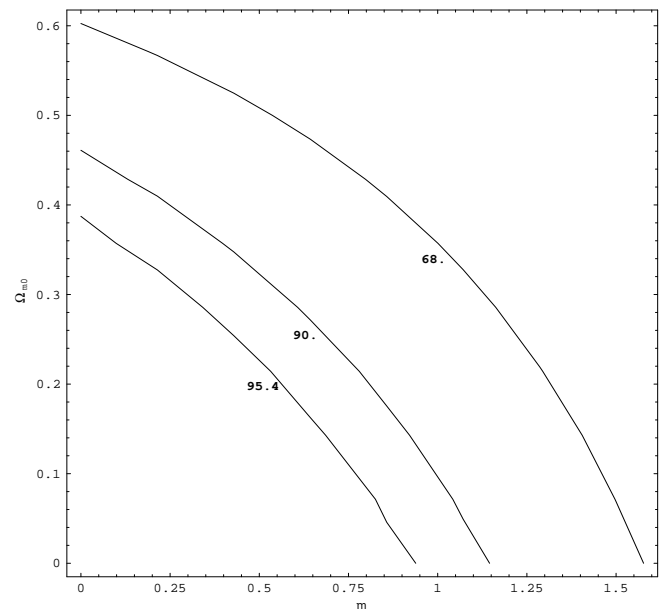


FIG. 3. Constraints imposed on the models by the magnitude-redshift test in which high- z SNe Ia are used as standard candles. The 95.4%, 90%, and 68% confidence levels on the parameters m and Ω_{m0} are shown in the figure.

In our computations we follow [15] and use the corrected B-magnitude intercept at $\Delta m_{15} = 1.1$ mag, $\mathcal{M}_{B,corr}^{\{1.1\}} = -3.32 \pm 0.05$, and consider only those 5 supernovae that have Δm_{15} values in the range 0.8 – 1.5 mag, which is the range of values investigated in the 18

low- z supernovae dataset. To construct the χ^2 we used the data points outer error bars of Perlmutter *et al.*, which are obtained by adding in quadrature the inner error bars of $m_{B,corr}$ (the apparent B-magnitude after width-luminosity correction) to $\sigma_{M_{B,corr}}^{Hamuy}$.

In Fig. 3 we plot the 95.4%, 90%, and 68% confidence levels for the parameters m and Ω_{m0} . We see that for the interesting range $\Omega_{m0} \gtrsim 0.2$, models with $m \gtrsim 1.3$ are in good agreement with the data. The goodness-of-fit (as defined in [15]) for the considered case is 0.59.

If we fix $m = 0$ we recover the result of Perlmutter *et al.* for constant Λ , $\Omega_{\Lambda} = 0.06_{-0.34}^{+0.28}$, with $\Omega_{\Lambda} < 0.51$ at the 95% confidence level (one tail). Another interesting case is $m = 2$. In this case we again have to consider one degree of freedom in $\Delta\chi^2 = \chi^2 - \chi_{min}^2$, and we find $\Omega_{m0} = 0.83_{-0.69}^{+0.82}$ (1σ) with goodness-of-fit equal to 0.75. So, models with $m = 2$ and $\Omega_{m0} > 0.14$ are also in good agreement with the data.

It is interesting to compare the above constraints with those arising from lensing statistics. In Fig. 4 we plot contours of constant likelihood (95.4%, 90%, and 68%) for the models, arising from lensing statistics. We used data from the HST Snapshot survey, the Crampton survey, the Yee survey, the ESO/Liege survey, The HST GO observations, the CFA survey, and the NOT survey [19]. We considered 859 ($z > 1$) quasars plus 5 lenses and to obtain the contours we adapted from [18] the procedure denoted there as “A2”.

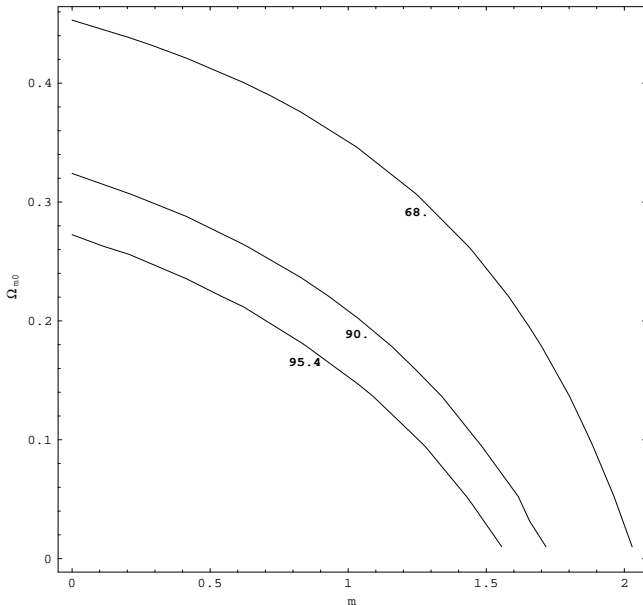


FIG. 4. Contours of constant likelihood (95.4%, 90% and 68%) arising from lensing statistics are shown.

By comparing Fig. 3 with Fig. 4 we see that the SNe Ia constraints are stronger for low values of m and Ω_{m0} ($m < 1$ and $\Omega_{m0} < 0.4$) while the lensing ones are more important for larger values of the parameter m ($m > 1$).

From Fig. 4 we observe that models with $\Omega_{m0} \gtrsim 0.2$ and $m \gtrsim 1.6$ are in good agreement with the data.

ACKNOWLEDGMENTS

It is a pleasure to thank Scott Dodelson, Josh Frieman, and Albert Stebbins for several useful discussions. Special thanks are due to Saul Perlmutter for kindly answering our questions and Chris Kochanek for sending us data on lensing surveys. This work was supported in part by the Brazilian agency CNPq and by the DOE and NASA at Fermilab through the grant NAGW-2381.

-
- [1] G.Efstathiou, W. J. Sutherland, and S. J. Maddox, *Nature (London)* **348**, 705 (1990).
 - [2] D. A. Vandenberg, M. Bolte, and P. B. Stetson, *Annu. Rev. Astron. Astrophys.* **34**, 461 (1996); see also, B. Chaboyer *et al.*, astro-ph 9706128, with new results based on recent Hipparcos parallax measurements which indicate younger ages ($\sim 10\%$ smaller) for the oldest globular clusters. If these results are confirmed the age problem will possibly be weakened. However, it is still early to say that the age crisis has gone away (see, e.g., W. L. Freedman, in astro-ph 9706072 for a recent discussion on this and related topics).
 - [3] N. R. Tanvir *et al.*, *Nature (London)* **377**, 27 (1995); W. Freedman, astro-ph/9612204; A. G. Riess, W. H. Press, and R. Kirshner, *Ap. J.* **438**, L17 (1995); M. Hamuy *et al.*, *Astron. J.* **112**, 2398 (1996).
 - [4] See, e.g., M. Ozer and M. O. Taha, *Nucl. Phys.* **B287**, 776 (1987); K. Freese *et al.*, *Nucl. Phys.* **B 287**, 797 (1987); M. Reuter and C. Wetterich, *Phys. Lett.* **B 188**, 38 (1987); B. Ratra and P. J. E. Peebles, *Phys. Rev.* **D 37**, 3407 (1988); I. Waga, *Ap. J.* **414**, 436 (1993); J. A. Frieman *et al.*, *Phys. Rev. Lett.* **75**, 2077 (1995); K. Coble, S. Dodelson, and J. A. Frieman, *Phys. Rev.* **D 55**, 1851 (1997).
 - [5] V. Silveira and I. Waga, *Phys. Rev.* **D 50**, 4890 (1994).
 - [6] W. Chen and Y. S. Wu, *Phys. Rev.* **D 41**, 695 (1990).
 - [7] For the models considered in this paper Ω_{Λ} is negligibly small during nucleosynthesis. However, this is not necessarily true for all Λ -decaying models present in the literature. For instance, for a class of models in which $\Omega_{\Lambda} = \beta = \text{constant}$, Freese *et al.* [4] showed that standard primordial nucleosynthesis constrains the parameter β to be $\beta \lesssim 0.1$.
 - [8] A. Vilenkin, *Phys. Rev. Lett.* **53**, 1016 (1984); D. N. Spergel and U. L. Pen, astro-ph/9611198; L. M. A. Bettencourt, P. Laguna and, R. A. Matzner, astro-ph/9612350.
 - [9] J. N. Fry, *Phys. Lett.* **B 158**, 211 (1985); V. Sahni, H. A. Feldman and A. Stebbins, *Ap. J.* **385**, 1 (1992); H. A. Feldman and A. E. Evrard, *Int. J. Mod. Phys.* **D 2**, 113

- (1993); J. Stelmach and M. P. Dabrowski, Nucl. Phys. **B 406**, 471 (1993); H. Martel, Ap. J. **445**, 537 (1995); P. J. Steinhardt, Nature (London), **382**, 768 (1996); M. S. Turner and M. White, astro-ph/9701138.
- [10] J. R. Bond and G. Efstathiou, Ap. J. **285**, L45 (1987); G. Efstathiou, Proc. Natl. Acad. Sci. USA **90**, 4859 (1993).
- [11] The evolution of modes bigger than the Hubble radius is described by the general relativistic equations [see, e. g., T. Padmanabhan, *Structure Formation in the Universe*, (Cambridge: Cambridge University Press), p. 141 - 146 (1993)]. Since nonrelativistic matter is conserved, and assuming that the x component is smooth the relativistic equation for $\delta\dot{H}$ may be written as an equation for $\delta_m(\vec{x}, t)$, giving us the same Newtonian equation used to describe the evolution of modes inside the horizon.
- [12] R. G. Sachs and A. M. Wolfe, Ap. J. **147**, 73 (1967).
- [13] P. J. E. Peebles, *Principles of Cosmology* (Princeton: Princeton University Press, 1993).
- [14] A. H. Jaffe, A. Stebbins, and J. A. Frieman, Ap. J. **420**, 9 (1994).
- [15] S. Perlmutter *et al.*, Ap. J. **483**, 565, (1997).
- [16] M. Hamuy *et al.*, A. J. **109**, 1 (1995); M. Hamuy *et al.*, A. J. **112**, 2391 (1996);
- [17] M. M. Phillips, Ap. J. **413**, L105 (1993).
- [18] L. F. Bloomfield Torres and I. Waga, Mon. Not. R. Astron. Soc. **279**, 712 (1996).
- [19] D. Maoz *et al.*, Ap. J. **409**, 28 (1993); D. Crampton, R. D. McClure, and J. M. Fletcher, Ap. J. **392**, 23 (1992); H. K. C. Yee, A. V. Filipenko, and D. H. Tang, A. J. **105**, 7 (1993); A. J. Surdej *et al.* **105**, 2064 (1993); E. E. Falco, in *Gravitational Lenses in the Universe*, edited by J. Surdej, D. Fraipont-Caro, E. Gosset, S. Refsdal, and M. Remy (Liege: Univ. Liege), 127 (1994); C. S. Kochanek, E. E. Falco, and R. Schild, Ap. J. **452**, 109 (1995); A. O. Jaunsen *et al.*, A & A **300**, 323 (1995).